Ultracold atoms in a cavity-mediated double-well system

Jonas Larson*
Department of Physics, Stockholm University, SE-106 91 Stockholm, Sweden

Jani-Petri Martikainen
NORDITA, SE-106 91 Stockholm, Sweden

(Received 21 June 2010; published 13 September 2010)

We study ground-state properties and dynamics of a dilute ultracold atomic gas in a double-well potential. The Gaussian barrier separating the two wells derives from the interaction between the atoms and a quantized field of a driven Fabry-Perot cavity. Due to intrinsic atom-field nonlinearity, several interesting phenomena arise which are the focus of this work. For the ground state, there is a critical pumping amplitude in which the atoms self-organize and the intra-cavity-field amplitude drastically increases. In the dynamical analysis, we show that the Josephson oscillations depend strongly on the atomic density and may be greatly suppressed within certain regimes, reminiscent of self-trapping of Bose-Einstein condensates in double-well setups. This pseudo-self-trapping effect is studied within a mean-field treatment valid for large atom numbers. For small numbers of atoms, we consider the analogous many-body problem and demonstrate a collapse-revival structure in the Josephson oscillations.

DOI: 10.1103/PhysRevA.82.033606 PACS number(s): 03.75.Lm, 42.50.Pq, 03.75.Nt

I. INTRODUCTION

Outcomes of nonlinearity have extensive consequences in various areas of physics leading to phenomena absent in their linear counterparts. In quantum mechanics, it plays a crucial role in fields such as nonlinear optics [1] and ultracold atomic gases [2]. In ultracold atomic gases, or Bose-Einstein condensates (BECs), the nonlinearity stems from interaction among the atoms, and causes effects such as insulating states of cold atoms in optical lattices [3], soliton and vortex formation [4], collapse-revivals of system evolution [5], or self-trapping of atoms in optical lattices or double-well (DW) systems [6]. Moreover, the inherent phase coherence of the BEC wave function has made it a good candidate for realizing analogs of the Josephson effect appearing across the bulk of two attached superconductors [7]. By placing the condensate in a DW potential, the weak tunneling through the center barrier brings about oscillations of the BEC between the two wells mimicking Josephson oscillation in superconductors [8]. Nonlinearity in the BEC DW system induces self-trapping and collapse-revivals in the Josephson current. Self-trapping emerges for large nonlinearity and large imbalance of atoms between the two wells and manifests itself as blocking of the Josephson oscillations. Collapse revivals characterize deaths and rebirths of the oscillations and become important in the quantum regime where fluctuations around the mean-field condensate order parameter become relevant.

In recent years, nonlinearity has turned out to be an essential ingredient in two different but highly linked matter-light quantum systems: optomechanical cavities [9] and BEC-cavity setups [10,11]. Here we focus on the second type in which pioneering experiments have demonstrated the square-root dependence on the number of atoms $\Omega_{\mathrm{Rabi}} \sim \sqrt{N}$ in the vacuum Rabi splitting [10]. Since then, most interest, both theoretical [12] and experimental [11,13], has indeed been paid to the intrinsic nonlinearity within the system manifested, for example, by optical bistability. In these systems, the cavity field acts as an effective potential for the atoms, but the atoms, in turn, induce a shift in the index of refraction altering the cavity field. As the field adjusts accordingly, the field causes a back action on the atoms, resulting in the nonlinear atom-field interplay. Apart from studies of bistability, research has considered also self-organization of ultracold atoms in optical resonators, either in setups of pumped cavities [14,15] or pumped atoms [16], as well as most recently simulation of the Dicke quantum phase transition [17].

In this paper, we focus on different outcomes of the atom-field nonlinearity compared to earlier works on optical bistability. That is, we are not mainly interested in multiple solutions of the equations of motion, but instead direct our attention to self-organization, self-trapping, as well as collapse-revivals in a cavity-mediated DW system. The appearance of additional solutions in nonlinear, in contrast to linear, systems is a quite general property. The present work therefore aims at more specific outcomes of atom-field nonlinearity. We notice that BEC DW systems coupled to cavity fields have been discussed previously [18,19], but those works did not analyze the situation in which the cavity field, and thereby the nonlinearity, drives the Josephson oscillations. Here, self-organization and self-trapping are analyzed in the mean-field regime, and our work goes beyond the two-mode approximations commonly utilized in DW analysis. We especially show, as for the BEC DW, that the atomic density affects the strength of nonlinearity, and thereby there is a critical atomic density at which an effective self-trapping behavior appears. Self-organization emerges when the pump amplitude exceeds a critical value. At the same instant, the intra-cavity-field amplitude greatly increases similarly to the pump threshold in the theory of laser. Within the mean-field approach, we also demonstrate how the system exhibits bistability as a result of nonlinearity. Collapse-revival structures derive from quantum fluctuations, and to tackle such effects we consider an effective two-mode many-body model for the system which indeed predicts such phenomena. We also

*jolarson@fysik.su.se

point out that the system setup automatically allows quantum nondemolition measurements of the atomic dynamics via the detection of the output cavity field.

II. JOSEPHSON OSCILLATIONS AND THE MODEL SYSTEM

Before describing the system of the present work, we briefly summarize the DW system in order to get a deeper understanding of the dynamics analyzed later on in the paper.

In the most simple situation, two wave functions $\psi_L(x)$ and $\psi_R(x)$ are coupled with some strength J. In the symmetric situation, the ground state and the excited state can be written as the symmetric and antisymmetric solutions

$$\begin{aligned}\Psi_0(x) &= \frac{1}{\sqrt{\mathcal{N}}}[\psi_L(x) + \psi_R(x)],\\ \Psi_1(x) &= \frac{1}{\sqrt{\mathcal{N}}}[\psi_L(x) - \psi_R(x)],\end{aligned} \tag{1}$$

where $\mathcal{N}$ is the proper normalization coefficient. In DW systems, J represents the tunneling coefficient and $\psi_{L,R}(x)$ are the normalized left well and right well wave functions as depicted in Fig. 1. In general, we can express the time-dependent solution $\Psi(x,t) = \phi_L(t)\psi_L(x) + \phi_R(t)\psi_R(x)$ leading to a set of two first-order coupled equations for $\phi_L(t)$ and $\phi_R(t)$. The corresponding Hamiltonian is

$$\hat{H}_{\text{Rabi}} = \begin{bmatrix} E_L & -J \\ -J & E_R \end{bmatrix}, \tag{2}$$

with $E_{L,R}$ the onsite energies of the left and right wells, and J the tunneling strength. Thus, in the symmetric well, the detuning $\delta = E_L - E_R$ vanishes. The Rabi frequency, characterizing the Josephson oscillations, is given by $\Omega_{\text{Rabi}} = 2\sqrt{J^2 + \delta^2}/\hbar$, which for the resonant well equals $2J/\hbar$. Nonzero detunings imply an increased Josephson period, as well as causing the amplitude of the inversion

$$\mathcal{Z} \equiv \frac{|\phi_R(t)|^2 - |\phi_L(t)|^2}{N} = 1 - \frac{8J^2}{\delta^2 + 4J^2}\sin^2(\Omega_{\text{Rabi}}t) \tag{3}$$

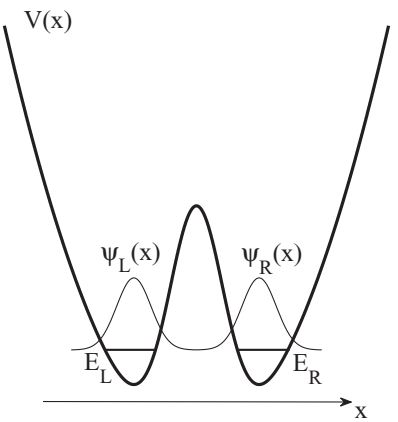

FIG. 1. Schematic picture of the traditional DW setup. In the symmetric DW, the two onsite energies E_L and E_R are equal. The left and right solutions are marked by $\psi_L(x)$ and $\psi_R(x)$, respectively.

to decrease from oscillating between -1 and 1 as in the case of zero detuning. In deriving (2), we have assumed $\mathcal{Z}(t=0) = 1$, i.e., all atoms initially in the right well.

A. Cavity-mediated double-well for cold atoms

In both BEC DW experiments of Ref. [20], the potential barrier separating the left and right wells is obtained by dispersive dipole interaction between the atoms and an external laser beam. The laser has a transverse Gaussian mode shape, whose width and amplitude are easily adjustable. The large laser intensity makes the light field approximately classical. By confining atoms in a resonator, the effective atom-field coupling can be greatly enhanced and thereby the dynamics of single atoms can be affected by the field even at average photon numbers less than unity [21]. For such low intensities, the light field sustained in the resonator must be treated quantum mechanically.

As we are dealing with a coupled bipartite quantum system, the state of the atoms will influence the state of the field and vice versa. Physically, the atomic-matter wave brings out a change in the index of refraction, and as the field adjusts to the new index of refraction, its change will in return affect the atoms leading to an intrinsic nonlinear atom-field interaction. For the present system, it implies that the effective DW potential directly depends on the atomic state.

The system we have in mind is illustrated in Fig. 2. A harmonic potential traps the atoms in all three dimensions, but the trap frequencies in the y and z directions are assumed large enough so that the atoms remain in their lowest vibrational states in these directions, and we consequently consider motion restricted to the x direction. Instead of an external laser, we consider the field of a cavity to constitute the tunneling barrier. To this end we use a Fabry-Perot cavity with its longitudinal axis along the y direction. As for a traditional laser beam, the Fabry-Perot cavity possesses TEM_{00} modes having transverse Gaussian profiles. The cavity has a large enough Q value to guarantee well-separated mode frequencies. Nonetheless, cavity losses κ are taken into account in all our derivations. Only a single cavity mode is quasiresonant with the atomic transition under consideration, and all other modes are therefore ignored. The cavity is externally driven with a classical field having amplitude η, and hence, without atoms present the cavity field would reach a steady state

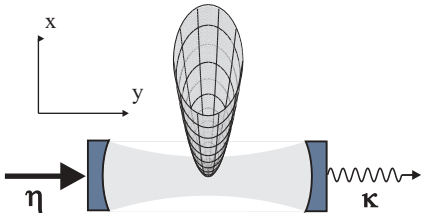

FIG. 2. (Color online) System setup. An anisotropic harmonic trap confines the atoms such that the motion can be considered quasi-one-dimensional along the x direction. The field of a Fabry-Perot cavity, aligned along the y direction, intersects the atomic trap. The TEM_{00}-mode shape of the cavity induces an effective Gaussian barrier separating the harmonic trap into two wells. Furthermore, the cavity is laser-driven through one end mirror with an amplitude η. Cavity losses, with decay rate κ, are marked by a curly arrow.

being coherent with an amplitude determined by the balancing of losses κ and pumping η. The cavity is taken to couple dispersively to the atoms, and the excited atomic state can hence be eliminated adiabatically [22]. In a frame rotating with the pump frequency ω_p and assuming ultracold atoms, the Hamiltonian reads [15]

$$\hat{H}_{\rm af} = -\hbar\Delta_c\hat{a}^\dagger\hat{a} - i\hbar\eta(\hat{a}-\hat{a}^\dagger) + \int dx\,\hat{\Psi}^\dagger(x)\left[-\frac{\hbar^2}{2m}\frac{\partial^2}{\partial x^2} + \frac{m\omega^2x^2}{2} + U(x)\hat{a}^\dagger\hat{a} + \frac{gN}{2}|\hat{\Psi}(x)|^2\right]\hat{\Psi}(x), \tag{4}$$

where $\Delta_c = \omega_p - \omega_c$ is the pump-cavity detuning, $\hat{a}^\dagger$ ($\hat{a}$) the photon creation (annihilation) operator obeying standard boson commutation rules, ω the trap frequency, and

$$U(x) = \hbar U_0\, e^{-\frac{x^2}{\Delta_x^2}} \tag{5}$$

is the effective dispersive atom-field coupling with $U_0 = \lambda^2/\Delta_a$, where λ is the single-photon atom-field coupling, $\Delta_a = \omega_p - \omega_a$ the pump-atom detuning, and Δ_x is the mode waist.

Note that to achieve a DW structure, we restrict the analysis to positive detunings, $\Delta_a > 0$, but interesting effects can also appear for negative detunings when the cavity field induces a potential "dimple" on the atoms and consequently raises the local phase-space density. In this work, choosing $U(x)$ centered around $x = 0$ we consider the symmetric DW, and consequently direct-current Josephson effect. The alternating-current Josephson effect is assessed by spatially shifting either the cavity or the trapping potential. The last nonlinear term on the right-hand side of Eq. (4) stems from atom-atom collisions and is generally proportional to the atomic density and the s-wave scattering length.

After introducing field losses κ, the corresponding Heisenberg-Langevin equations become

$$\begin{aligned}\frac{d}{dt}\hat{a} &= -(\kappa - i\Delta_c)\hat{a} + \eta - iN\int|\hat{\Psi}(x)|^2U(x)\,dx\,\hat{a} + \sqrt{2\kappa}\hat{a}_{\rm in}(t),\\ \frac{d}{dt}\hat{\Psi}(x) &= \left[-\frac{\hbar^2}{2m}\frac{\partial^2}{\partial x^2} + \frac{m\omega^2x^2}{2} + U(x)\hat{a}^\dagger\hat{a} + gN|\hat{\Psi}(x)|^2\right]\hat{\Psi}(x).\end{aligned} \tag{6}$$

Here, $\hat{a}_{\rm in}(t)$ is the Langevin field input noise source being δ correlated; $\langle\hat{a}_{\rm in}(t)\hat{a}_{\rm in}(t')^\dagger\rangle = \delta(t-t')$, and $\langle\hat{a}_{\rm in}^\dagger(t)\hat{a}_{\rm in}(t')\rangle = \langle\hat{a}_{\rm in}(t)\rangle = 0$ otherwise [23]. In the present work, the influence of quantum noise will be assumed small and hereafter neglected. The effects of such fluctuations in a BEC cavity system similar to the one we study have been analyzed in Ref. [24].

In typical experiments, the characteristic time scales for the field and atoms are substantially different [10]. The field evolution can be assumed to follow the dynamics of the atoms, and it is therefore justified to consider the steady-state solutions of the field. Explicitly, the steady state for the photon number $\hat{n} = \hat{a}^\dagger\hat{a}$ is given by

$$\hat{n}_{\rm ss} = \frac{\eta^2}{\kappa^2 + (\Delta_c - N\hat{Y})^2}, \tag{7}$$

with the operator $\hat{Y} = \int|\hat{\Psi}(x)|^2U(x)\,dx$. This equation makes clear the modification of the detuning Δ_c induced by the atoms, i.e., the resonance condition $\Delta_c = 0$ is shifted to $\Delta_c = N\hat{Y}$. Since the atomic field $\hat{\Psi}(x)$ is coupled to the atom number $\hat{n}$, it follows that so is $\hat{Y}$, and then Eq. (7) may render multiple solutions of the photon number. This same nonlinear effect give rise to quantum optical bistability [12,13], which can furthermore be shown to be analogous to bistable optomechanics in certain regimes [11].

The intrinsic atom-field nonlinearity is rather different from the nonlinearity originating from atom-atom interactions [25]. The number of photons enters in the effective system potential, and since it depends on the matter state, the effective potential can be seen as a dynamical variable. In the BEC DW situation, nonlinearity enters in the atom-atom interaction term, and within the Thomas-Fermi regime (where kinetic energies can be neglected) it can be viewed as changing the chemical potentials in the two wells. Roughly speaking, as an outcome in the BEC DW, the effective shift due to nonlinearity enters in the detuning δ; while in the cavity DW, it modifies the field strength $\hat{n}_{\rm ss}$ and thereby the tunneling coefficient J.

Throughout, we try to use realistic experimental parameters. More explicitly, we consider the cavity decay rate κ from the experiment of the Esslinger group [13] and express other rates in terms of this. Length scales as well as atom numbers are taken to be experimentally realistic.

III. STATIONARY SOLUTIONS

In this and the next section, we discuss the system at a mean-field level, i.e., replacing the atomic operator $\hat{\Psi}(x)$ by its mean. The resulting Gross-Pitaevskii equation [26]

$$i\frac{d}{dt}\Psi(x) = \left[-\frac{\hbar^2}{2m}\frac{\partial^2}{\partial x^2} + \frac{m\omega^2x^2}{2} + n_{\rm ss}U(x) + gN|\Psi(x)|^2\right]\Psi(x) \tag{8}$$

for the order parameter can be solved for the minimum energy solution by propagating it in imaginary time and updating the cavity photon number

$$n_{\rm ss} = \frac{\eta^2}{\kappa^2 + (\Delta_c - NY)^2} \tag{9}$$

during the propagation so that it corresponds to the instantaneous steady-state photon number. Here Y is the mean-field counterpart of the operator $\hat{Y}$. The corresponding energy functional is given by [25]

$$\frac{E[\Psi]}{N} = \int\left[\left(\frac{\hbar^2}{2m}\right)\left|\frac{\partial\Psi(x)}{\partial x}\right|^2 + \frac{m\omega^2x^2}{2}|\Psi(x)|^2 + \frac{gN}{2}|\Psi(x)|^4\right]dx - \frac{\eta^2}{\kappa N}\arctan\left(\frac{\Delta_c - N\int U(x)|\Psi(x)|dx}{\kappa}\right). \tag{10}$$

In this paper we are not interested in the interaction effects due to atomic collisions, but wish to focus on the coupling between the cavity mode and the atoms. Therefore, we chose $g = 0$ which can be achieved via Feshbach resonances [27] or is approximately valid in a sufficiently dilute gas.

While a direct solution of the Gross-Pitaevskii equation is relatively easily found numerically, we found that in many instances most of the equilibrium physics (and some of the dynamics as well) can also be captured by a more transparent variational ansatz. Our ansatz is a Gaussian ansatz which can have two peaks, namely,

$$\psi(x) = C\left[e^{-\frac{(x+x_0)^2}{2\sigma^2}} + e^{-\frac{(x-x_0)^2}{2\sigma^2}}\right], \tag{11}$$

where the prefactor is set by the normalization $\int dx|\psi(x)|^2 = 1$ and is given by

$$C = \frac{1}{\pi^{1/4}\sqrt{2\sigma^2\left\{1+\exp\left[-\left(\frac{x_0}{\sigma}\right)^2\right]\right\}}}. \tag{12}$$

Substituting this ansatz into the energy functional gives us an energy functional $E(\sigma,x_0)$ which can be minimized to find the optimal solution. All integrals are sufficiently easy to solve analytically, but the resulting expressions are too long to be given here explicitly.

The steady-state solutions naturally separate into two different regimes: one at the low values of the pumping strength and the other at large pumping strengths. When the pumping strength is small, the atomic order parameter is nearly a Gaussian centered around the origin. In this limit, the atomic density overlaps strongly with the Gaussian cavity mode function, and if the coupling strength U_0 is quite large, Y can be substantial. Then the steady-state photon number can be suppressed by the NY term appearing in the denominator of Eq. (9) if $|NY| \gg \Delta_c$. As the pumping is increased, the photon number increases at first roughly $\propto \eta^2$ followed by a pronounced jump in the cavity photon number at some critical pump strength.

This jump coincides with a qualitative change in the atomic order parameter as the atomic density splits into two separate peaks and develops a minimum at the origin. This transition is signaled by a rapid increase in the cavity photon number, since the overlap of the atomic density and the cavity mode function is rapidly reduced so that the NY contribution in the steady-state photon number becomes less important. At the same time, the effective potential experienced by the atoms becomes a stronger double-well potential, which pushes the atomic density peaks farther apart and lowers the overlap with the cavity mode function even more. In a way, as one increases the pumping, one can move from a regime where coupling between the atomic order parameter and cavity field is strong into a regime where it is weak and the cavity field mainly acts as an independent optical potential acting on the atoms.

This drastic change in the atomic density of the ground state is an example of self-organization [16,28]. If the atoms are externally pumped, rather than the cavity field, the atoms act as a scatter which transfers photons from the pump into the resonator. Thereby, there is a direct resemblance between pumping of the atoms and pumping of the cavity field. The corresponding phenomenon for pumped atomic systems has been studied in great detail, and it was found that the transition is described by a second-order phase transition [29]. The same behavior reminds us of threshold pumping of lasers. Pumping of the laser must exceed a critical value in order for lasing to set off. Again, such a critical structure has been identified as a second-order phase transition [30]. Moreover, it is worth pointing out that in a very recent experiment, the same kind of transition was demonstrated for a driven lossy cavity in circuit QED [31].

The critical pump strength which separates these two self-organized regimes occurs roughly when the barrier height becomes larger than the energy scale of the background harmonic oscillator i.e., when $n_{ss}\hbar U_0 \sim \hbar\omega$. The resonance in the photon number occurs when $\Delta_c = NY$. For the Gaussian ground state of the noninteracting system (which is accurate at small pump strengths), this implies $NU_0/\Delta_c = \sqrt{1+\sigma/\Delta_x^2}$, where $\sigma = \sqrt{\hbar/m\omega}$ is the width of the noninteracting (Gaussian) atomic wave function. In this paper we mostly use $\Delta_x = \sigma/2$.

In Fig. 3, we show an example of the behavior of the steady-state photon number as a function of pumping, together with a few examples of the associated atomic order parameters as obtained from imaginary time propagation of the Gross-Pitaevskii equation. In this figure, we also compare the double-peaked Gaussian ansatz with the results from the Gross-Pitaevskii equation and find the agreement to be very good. Using the Gaussian ansatz we can, depending on parameters, find two stationary solutions corresponding to minima of the energy functional. The upper branch is the global minimum, while the lower one is locally stable.

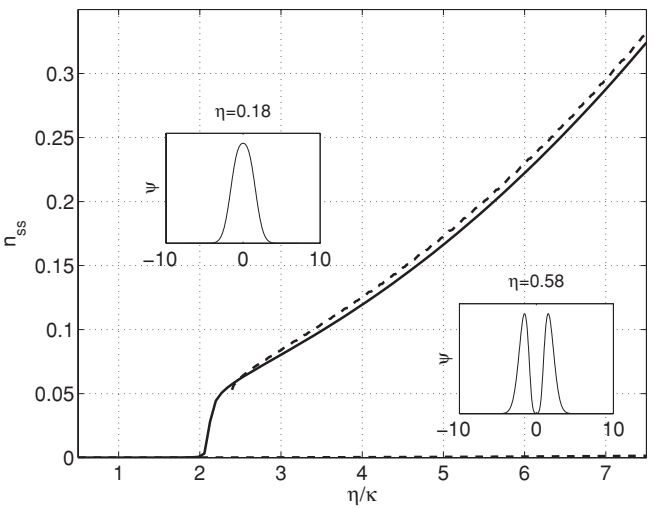

FIG. 3. The mean-field photon number as a function of η/κ using a double-peaked Gaussian ansatz (dashed line) and Gross-Pitaevskii approach (solid line). With some parameters, the Gaussian ansatz predicts an existence of two stationary solutions corresponding to local minima. Both of these solutions are indicated in the figure. Insets show the wave-function amplitude $|\Psi(x,t)|$ using the Gross-Pitaevskii equation at both smaller and higher pumping strengths. We used parameters $N = 10\,000$, $\kappa = 2\pi \times 1.3$ MHz, $\Delta_c = \kappa$, $U_0 = \kappa/100$, $\Delta_x = 0.5\sqrt{\hbar/m\omega}$, $\omega = \kappa/500$, and $m = 87u$.

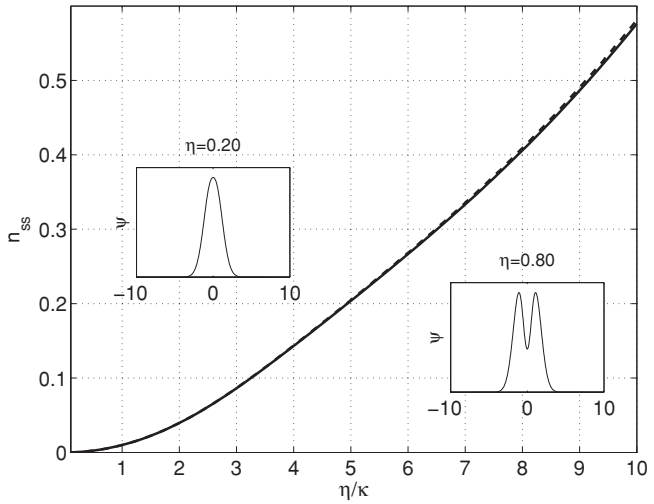

FIG. 4. n_{ss} using a double-peaked Gaussian ansatz (dashed line) and Gross-Pitaevskii approach (solid line). Insets show the wave-function amplitude $|\Psi(x,t)|$ using the Gross-Pitaevskii equation at both smaller and higher pumping strengths. We used parameters $N = 10\,000$, $\kappa = 2\pi \times 1.3$ MHz, $\Delta_c = \kappa$, $U_0 = \sqrt{5}\kappa/N \approx 0.000224\,\kappa$, $\Delta_x = 0.5\sqrt{\hbar/m\omega}$, $\omega = \kappa/500$, and $m = 87u$.

Our Gross-Pitaevskii approach only finds the global minimum, and in order to find the other solution, we would have to impose additional constraints on the imaginary time propagation.

In agreement with earlier works on atom-light bistability [12,13], the present model supports two or one stable values of n_{ss}. In addition to these solutions, there exists the "middle" branch of the hysteresis curve representing an unstable solution corresponding to a local energetic maximum. We have not plotted this branch in Fig. 3.

The above discussion is based on a fairly high value ($U_0 = \kappa/100$) of atom-field coupling. For a lower value of U_0 the behavior can be quite different. As an example, we show in Fig. 4 results using the double-peaked Gaussian ansatz and the Gross-Pitaevskii approach with otherwise the same parameters, but a much smaller coupling $U_0 \approx 0.000224\kappa$. We chose this value because then $\Delta_c - NY = 0$ and the steady-state photon number is on resonance for the ideal gas Gaussian ground state, when other parameters are kept the same as in Fig. 3. In this case, the large overlap between the atomic order parameter and the cavity mode function enhances the steady-state photon number. This is in contrast to the behavior at larger couplings, where similar large overlap implied strong suppression of the cavity photon number. In this case, we can find no evidence of bistability, and the double-peaked atomic order parameter appears smoothly as the pumping strength is increased. At the same time the overlap between the cavity mode function and the atomic density decreases smoothly.

IV. MEAN-FIELD DYNAMICS

In this section we give an overview of the typical features of the system dynamics at the mean-field level. Precise details naturally vary based on the parameters used, but the basic

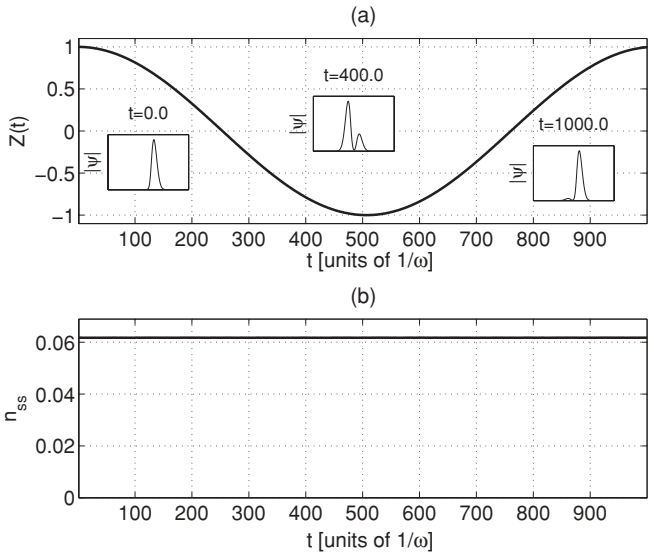

FIG. 5. Dynamics of the atomic order parameter when the initial state was localized to the right of the cavity mode barrier. Figure (a) shows the inversion $\mathcal{Z}(t)$ together with few snapshots of the absolute value $|\Psi(x,t)|$ of the atomic order parameter. Plot (b) displays the photon number n_{ss}. We used parameters $N = 10\,000$, $\kappa = 2\pi \times 1.3$ MHz, $\eta = 25\,\kappa$, $\Delta_c = \kappa$, $U_0 = \kappa/200$, $\Delta_x = 0.5\sqrt{\hbar/m\omega}$, $\omega = \kappa/500$, and $m = 87u$.

structures and the physical picture behind them is robust with respect to changes in the parameters.

We can construct wave packets which are localized either left or right of the barrier by finding the symmetric $[\psi_{\rm sym}(x)]$ and antisymmetric solutions $[\psi_{\rm asym}(x)]$ to the Gross-Pitaevskii equation. Using these solutions, the orthogonal solutions localized either to the left or right are given by

$$\psi_L(x) = [\psi_{\rm sym}(x) - \psi_{\rm asym}(x)]/\sqrt{2} \tag{13}$$

and

$$\psi_R(x) = [\psi_{\rm sym}(x) + \psi_{\rm asym}(x)]/\sqrt{2}. \tag{14}$$

In Fig. 5, we present an example of the dynamics for an initial state which is localized to the right of the barrier. Since the barrier height in this case is quite high, the overlap between the mode function and the order parameter is small. This remains true even in the course of the dynamics, and the cavity photon number has only weak time dependence. The atomic order parameter then exhibits Rabi-flopping from the right localized state to the left localized state with a period which becomes longer as the barrier gets higher and/or the cavity mode function wider. Plotted is the inversion

$$\mathcal{Z}(t) = 1 - 2\int_{-\infty}^{0} |\Psi(x,t)|^2\, dx, \tag{15}$$

and the photon number (9). For the utilized parameters, $t = 100$ in dimensionless variables corresponds to approximately 6 ms.

In Fig. 6, we show another example of the dynamics for an initial state which is localized to the right of the barrier, but with a smaller U_0 and larger Δ_c. In this case, the cavity photon number does have pronounced time dependence, and

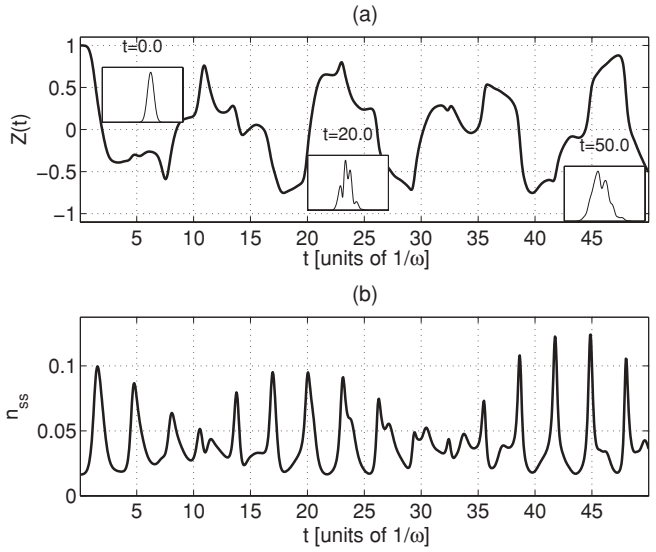

FIG. 6. Dynamics of the atomic order parameter when the initial state was a Gaussian localized at $x_0 = 2$ to the right of the cavity mode barrier and having a width $\sigma = 0.8$. Figure (a) shows the inversion $\mathcal{Z}(t)$ together with few snapshots of the absolute value $|\Psi(x,t)|$ of the atomic order parameter, while (b) gives the photon number n_{ss}. We used parameters $N = 10\,000$, $\kappa = 2\pi \times 1.3$ MHz, $\eta = 40\kappa$, $\Delta_c = 3\kappa$, $U_0 = \Delta_c\sqrt{5}/N$, $\Delta_x = 0.5\sqrt{\hbar/m\omega}$, $\omega = \kappa/500$, and $m = 87u$.

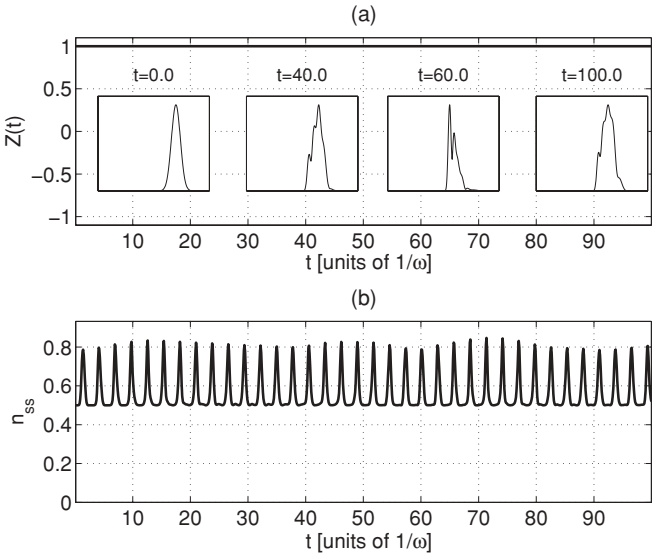

FIG. 7. Dynamics of the atomic order parameter when the initial state was an excited state with a Gaussian profile localized to the right of the cavity mode barrier. Figure (a) shows the inversion $\mathcal{Z}(t)$ together with a few snapshots of the absolute value $|\Psi(x,t)|$ of the atomic order parameter. Within the time period of this plot, the atoms are localized within the right well, i.e., pseudo-self-trapped. (b) displays the photon number n_{ss}. We used parameters $N = 10\,000$, $\kappa = 2\pi \times 1.3$ MHz, $\eta = 100\kappa$, $\Delta_c = \kappa$, $U_0 = \kappa/200$, $\Delta_x = 0.5\sqrt{\hbar/m\omega}$, $\omega = \kappa/500$, and $m = 87u$.

the system cannot be described as a simple Rabi-flopping anymore. The reason for the dramatically different dynamics is that with the parameters used in Fig. 6, the initial barrier height is quite low and proportional to $1/(\kappa^2 + \Delta_c^2)$ since the overlap between the atomic density and the cavity mode is low. This low barrier height enables the wave function to populate also the barrier region to a greater extent, which increases the overlap with the cavity mode. However, such increase lowers the $(\Delta_c - NY)^2$ term in the denominator of Eq. (9) and causes the photon number to increase toward its maximum value $\propto 1/\kappa^2$. This increase in turn increases the barrier height, which tends to drive the atomic order parameter away from the region close to the origin. A final result of this complicated interplay is a pronounced correlated dynamics of the atoms and the cavity field. The cavity field reaches a maximum when atoms are, on the average, more closely located to the center and is a minimum when the order parameter has only a small overlap with the cavity mode.

It should be noticed that while the results in Fig. 5 can be analyzed using a two-mode description [6], the results presented in Fig. 6 cannot be analyzed in that way and a multimode description is essential. Since the field amplitude is proportional to the photon number, detection of the output-cavity-field intensity would directly reveal some properties of the atom dynamics in the cavity. Moreover, such recording of the output cavity field is nondestructive. The idea of utilizing dispersive cavity interaction for nondemolition measurements has been discussed in terms of BEC DW systems [19] and for cold atoms trapped in optical lattices [32]. These references, however, do not consider the cavity field as supplying an effective potential and thus the systems studied are very different from the present system.

When the system was prepared in a localized state whose energy is close to the ground state of the double-well potential, we found a simple Rabi flopping behavior in Fig. 5. In Fig. 7, we demonstrate how the state can become effectively localized to the one side of the double-well system when it is prepared in a localized excited state. Here we prepared the atoms in a displaced Gaussian state and let the system evolve with somewhat higher cavity pumping strength than in Fig. 5. As the atoms approach the barrier region, the photon numbers rise, make the barrier higher, and tend to push the atoms back. In this case, the atoms effectively stay localized in one well, and the cavity photon number has a regular variation which reflects the average position of the atoms in a DW system. In this respect, the localization is reminiscent of self-trapping. In regular BEC DW systems, increasing the atom number implies enhanced nonlinearity and a transition between delocalized to localized states. This pseudo-self-trapping is not perfect; the tunneling rate becomes very small but it is still finite, while in BEC DW systems it is rather the detuning that is affected by the nonlinearity and therefore the oscillations are never perfect in this case. Note, however, that within typical experimental time scales, one would expect well-established localization.

In finding the steady-state solution to the Gross-Pitaevskii equation using the imaginary time propagation, we converged to the state corresponding to the upper branch of the Gaussian ansatz and ignored the other stationary state. However, even if this state is not the lowest energy state, it can play an important role in the dynamical behavior of the atoms. We illustrate this with few examples in Figs. 8 and 9. In Fig. 8 we start from the steady state at small pumping strengths and then ramp it

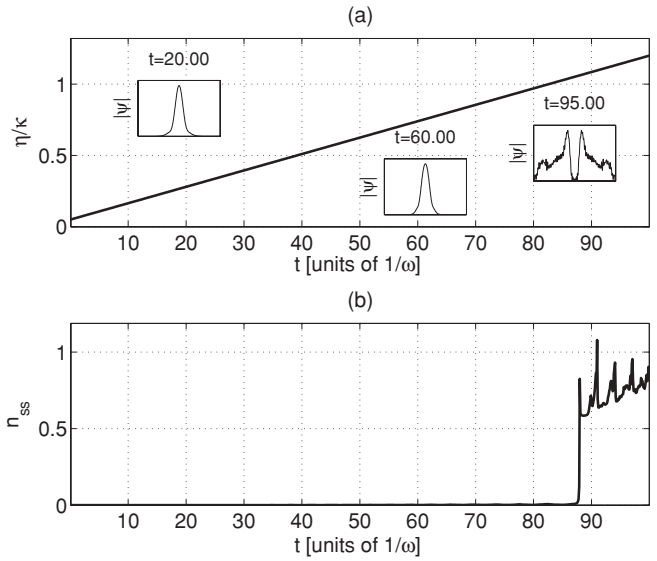

FIG. 8. The pump strength (a), mean-field photon number (b), and snapshots (insets) of the atomic order parameter $|\Psi(x,t)|$ as a function of time when the pump strength is swept from low to high values. After a certain pump strength, the barrier separating the left and right wells becomes sufficiently large to split the atom density and simultaneously the photon number makes a drastic change. We used parameters $N = 10\,000$, $\kappa = 2\pi \times 1.3$ MHz, $\Delta_c = \kappa$, $U_0 = \kappa/200$, $\Delta_x = 0.5\sqrt{\hbar/m\omega}$, $\omega = \kappa/500$, and $m = 87u$.

up, while in Fig. 9 we do the reverse. Comparing the results indicates a hysteresis type of behavior.

When the pumping field is ramped up, at first very little happens either for the atomic order parameter or the cavity field. There is a broad range of pumping strength above the critical pumping strength for the transition to a double-peaked atomic density distribution where the system is still dynamically, but not thermodynamically, stable. Only when the pumping strength exceeds some higher threshold does the system become dynamically unstable. When this happens, the atomic order parameter quickly splits, the cavity photon number is suddenly increased, and the energy of the atoms is increased considerably in this abrupt process.

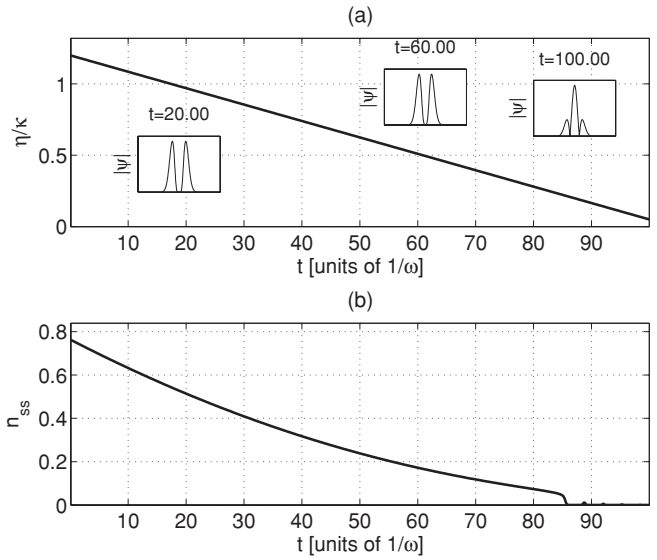

FIG. 9. Same as Fig. 8, but when the pump strength is swept from high to low values. In comparison to Fig. 8, the transition here is much smoother. .

This behavior is easy to understand, since here we start with a single-peaked atomic order parameter which has a substantial overlap with the cavity mode function. This means that the photon numbers, and hence the barrier height, are strongly suppressed by the NY term in the denominator. Only once the pumping strength becomes so strong that the barrier height is increased sufficiently to split the wave function, does the picture change. Then the overlap parameter Y is quickly reduced and the photon number (and the barrier height) increases. This in turn splits the atomic order parameter even more and results in the abrupt dynamics we observe.

On the other hand, when the field is ramped down (Fig. 9) the initial order parameter has only small overlap with the cavity mode function. Reducing the pumping strength will then reduce the barrier height smoothly allowing the order parameter to contracts toward the single peaked order parameter more smoothly. Eventually the overlap between the order parameter and the cavity mode becomes so strong that the NY term in the denominator of Eq. (9) reduces the photon number more strongly than the simple reduction of the pumping strength would suggest.

Up to now we considered an atom number $N = 100$ which is of the correct order of magnitude with present experiments [10]. The thermodynamical limit is given by letting N and the effective mode volume V tend to infinity while keeping the density $\rho = N/V$ fixed. In the driven cavity QED system, one has $U_0 \propto V^{-1}$ and $\eta \propto \sqrt{V}$ [33], and it follows that the effective potential $n_{\rm ss}U(x)$ depends solely on ρ, not N and V independently. Consequently, the same characteristics are obtainable for other atom numbers N by suitably choosing η and U_0.

V. DYNAMICS BEYOND MEAN FIELD

Since it is known that often the relevant physics can be captured by a two-mode model, we consider such an approach in this section which in particular allows us to explore physics beyond the mean field. Especially for deep enough DWs, it is legitimate to assume that the ground state can be written as in Eq. (1), i.e., $\Psi_0(x) = \frac{1}{\sqrt{2}}[\psi_L(x) + \psi_R(x)]$ with $\psi_{L,R}(x)$ localized states in the left and right wells. As in the previous sections, the left and right functions $\psi_{L,R}(x)$ are taken to be Gaussian in form. We pick the center of these to coincide with the minima of the effective potential

$$V_{\rm eff}(x) = \frac{m\omega^2 x^2}{2} + U(x)n_{\rm ss}, \tag{16}$$

giving

$$x_0 = \Delta_x \sqrt{\ln\left(\frac{2\hbar U_0 n_{\rm ss}}{\Delta_x^2 m\omega^2}\right)}. \tag{17}$$

The width, on the other hand, is obtained from minimizing the corresponding energy functional. In principle, x_0 could be kept a variational parameter, but to simplify the estimations of the parameters of our two-mode model, we impose this additional

assumption. Relaxing this constraint is straightforward but is not expected to change our results in an important way, especially when the barrier height is large compared to the energy scale of the harmonic trap.

Thus, the width σ is found by minimizing the system's energy functional. This results in a set of coupled nonlinear equations for σ and n_{ss} which must be solved self-consistently. In particular, multiple solutions of the equations may exist in certain parameter regimes. Introducing the overlap integrals

$$\begin{aligned} E_0 &= -\frac{\hbar^2}{2m}\int \psi_i^*(x)\left(\frac{d^2}{dx^2}\right)\psi_i(x)\,dx, \\ E_1 &= -\frac{\hbar^2}{2m}\int \psi_L^*(x)\left(\frac{d^2}{dx^2}\right)\psi_R(x)\,dx, \\ J_0 &= \int |\psi_i(x)|^2 e^{-x^2/\Delta_x^2}\,dx, \\ J_1 &= \int \psi_L^*(x)\psi_R(x)e^{-x^2/\Delta_x^2}\,dx, \\ S_0 &= \frac{m\omega^2}{2}\int |\psi_i(x)|^2 x^2\,dx, \\ S_1 &= \frac{m\omega^2}{2}\int \psi_L^*(x)\psi_R(x)x^2\,dx, \end{aligned} \tag{18}$$

the ground-state energy within the present ansatz takes the form [25]

$$\begin{aligned} \frac{E}{N} &= E_0 + E_1 + S_0 + S_1 \\ &\quad - \frac{\eta^2}{\kappa N}\arctan\left(\frac{\Delta_c - U_0 N(J_0+J_1)}{\kappa}\right). \end{aligned} \tag{19}$$

We artificially impose orthogonality of the left and right well wave functions [$\int \psi_L^*(x)\psi_R(x)\,dx = 0$] in order to avoid unphysical contributions, and then we get

$$\begin{aligned} E_0 &= \frac{\hbar^2}{4m\sigma^2}, \quad E_1 = \frac{\hbar^2}{4m\sigma^2}e^{-\frac{x_0^2}{\sigma^2}}, \\ J_0 &= \frac{\Delta_x}{\sqrt{\Delta_x^2+\sigma^2}}e^{-\frac{x_0^2}{\Delta_x^2+\sigma^2}}, \quad J_1 = \frac{\Delta_x}{\sqrt{\Delta_x^2+\sigma^2}}e^{-\frac{x_0^2}{\sigma^2}}, \\ S_0 &= \frac{m\omega^2}{2}\left(x_0^2+\frac{\sigma^2}{2}\right), \quad S_1 = \frac{m\omega^2}{2}\frac{\sigma^2}{2}e^{-\frac{x_0^2}{\sigma^2}}. \end{aligned} \tag{20}$$

As pointed out, in order to analyze effects beyond mean field, we assume the system parameters to be such that we can impose a two-mode approximation. Thus, we expand the atomic operators as $\hat{\Psi}(x) = \hat{b}_L\psi_L(x) + \hat{b}_R\psi_R(x)$, where $\hat{b}_{L,R}$ ($\hat{b}_{L,R}^\dagger$) annihilates (creates) an atom in well L, R, and $\psi_{L,R}(x)$ are determined as above. The two functions $\psi_{L,R}(x)$ are operator valued, since they depend on the cavity-field amplitude. As an outcome, in deriving equations of motion or an effective Hamiltonian for the atoms when the cavity field is eliminated, one has to take ordering between noncommuting operators into account [15]. To do so, we will assume $J_0 \gg J_1$ and leave out the J_1 cross term in $\hat{Y}$ for the steady-state photon number of Eq. (7). For the present potential $U(x)$, this is not always justified, but nevertheless it holds in large-parameter regimes. In this work, we will not present the full derivation of the effective Hamiltonian, but the reader can refer to Ref. [15] for details. To order $1/N^2$, we find a second quantized Hamiltonian for the atoms

$$\hat{H}_{\rm BH} = (E_0+S_0)\hat{N} + f(\hat{N}) - t(\hat{N})\hat{B}, \tag{21}$$

where

$$\begin{aligned} \hat{N} &= \hat{n}_R + \hat{n}_L = \hat{b}_R^\dagger\hat{b}_R + \hat{b}_L^\dagger\hat{b}_L, \\ \hat{B} &= \hat{b}_R^\dagger\hat{b}_L + \hat{b}_L^\dagger\hat{b}_R, \\ t(\hat{N}) &= -E_1 - S_1 - \frac{\hbar\eta^2 U_0 J_1}{\kappa^2 + (\Delta_c - U_0 J_0\hat{N})^2}, \\ f(\hat{N}) &= \frac{\hbar\eta^2}{\kappa}\arctan\left(\frac{\Delta_c - U_0 J_0\hat{N}}{\kappa}\right), \end{aligned} \tag{22}$$

and the coefficients are given in Eq. (20).

Transforming the operators as

$$\begin{bmatrix} \hat{b}_+ \\ \hat{b}_- \end{bmatrix} = \frac{1}{\sqrt{2}}\begin{bmatrix} 1 & 1 \\ 1 & -1 \end{bmatrix}\begin{bmatrix} \hat{b}_L \\ \hat{b}_R \end{bmatrix} \tag{23}$$

the Hamiltonian is diagonalized

$$\hat{H}_{\rm BH} = (E_0+S_0)\hat{N} + f(\hat{N}) - t(\hat{N})(\hat{n}_+ - \hat{n}_-), \tag{24}$$

with the new number operators $\hat{n}_+ = \hat{b}_+^\dagger\hat{b}_+$ and $\hat{n}_- = \hat{b}_-^\dagger\hat{b}_-$. For given atom number N, there are $N+1$ equidistant energy levels separated by $t(N)$. In this case, we recover perfect Josephson oscillations with an oscillation frequency $\Omega_{\rm Rabi}(N) = 2|t(N)|/\hbar$. For atomic states with an uncertain number of atoms, the various N's will induce a collapse in the Josephson oscillations as the contributing terms move out of phase. Such a collapse was discussed for the regular BEC DW in Ref. [5], where it derives from the atom-atom interaction term. For moderate or large atom numbers, it is appropriate to assume an initial coherent atomic state

$$|\psi\rangle = e^{-\bar{N}/2}\sum_n \frac{\bar{N}^{n/2}}{\sqrt{n!}}|n,0\rangle. \tag{25}$$

Here, $\bar{N} = \langle\hat{N}\rangle$ is the average number of atoms and the state $|n,m\rangle$ gives the number n of atoms in the left well and m atoms in the right well. For $\bar{N}\to\infty$, the relative uncertainty $\delta N = \Delta N/\bar{N}$, where $\Delta N = \langle(\hat{N}-\bar{N})^2\rangle$, goes to zero representing the "classical" (mean-field) limit. Depending on the particular N dependence of $t(N)$, the different Josephson oscillation terms may return in phase causing the system to revive [5]. The revival time T_r can be estimated as the time it takes for consecutive terms to build up a 2π phase difference $T_r[\omega_J(\bar{N}+1) - \omega_J(\bar{N})] = 2\pi$ giving

$$T_r \approx \pi\hbar\left(\frac{\partial t(N)}{\partial N}\bigg|_{N=\bar{N}}\right)^{-1}. \tag{26}$$

The N dependence of $t(N)$ is supposedly weak in the large atom limit implying $T_r\to\infty$ as $N\to\infty$, as expected in the classical limit. Collapse-revival patterns are a widespread phenomena in physics and have especially been studied in the vibrational dynamics of molecules [34] and in cavity QED [33], as direct proofs of quantization of either the molecular vibrations or the electromagnetic field. In the BEC DW system, the collapse-revivals derive from the squared atom number

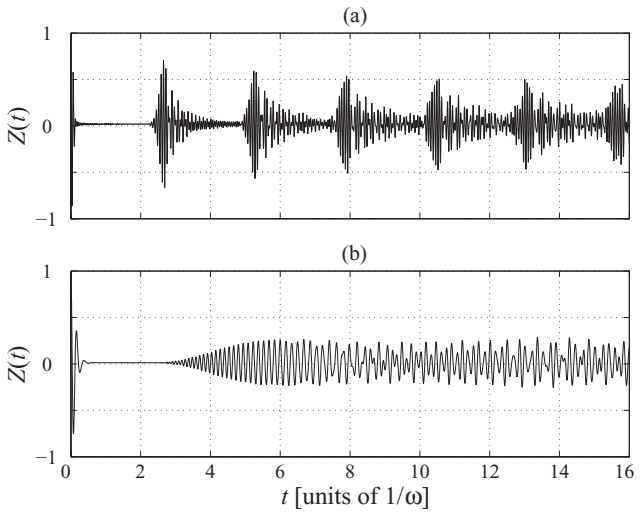

FIG. 10. Time evolution of the inversion $\mathcal{Z}(t)$ for an initial coherent state in the right well with $\bar{N} = 50$ (a) and $\bar{N} = 100$ (b). The common parameters are $\kappa = 2\pi \times 1.3$ MHz, $\Delta_c = \kappa$, $\eta = 2\kappa$, $U_0 = \kappa/5$, $\Delta_x \approx 0.1\ \mu m$, and $\omega = \kappa/500$.

operators, $\hat{n}^2_{L,R}$, while in standard cavity QED it is typically an outcome of a square-root dependence of photon numbers in the Jaynes-Cummings model [35], $\sqrt{\hat{n}}$. Here, the atom number dependence of $t(N)$ is presumably more complex, and one thereby expects a less pronounced collapse-revival structure.

In Fig. 10, we display the time evolution of the many-body inversion

$$\mathcal{Z}_{\rm mb} = \frac{\langle \hat{n}_R \rangle - \langle \hat{n}_R \rangle}{\bar{N}} \tag{27}$$

for an initial coherent atomic state in the right well with $\bar{N} = 50$ (a) and $\bar{N} = 100$ (b). At short times, $t < 0.3$, a few Josephson oscillations persist before the collapse. The collapse time is approximately the same for both examples, which is a general property [33]. The first collapse period lasts until $t \sim 2.7$ for $\bar{N} = 50$ and until $t \sim 3.2$ for $\bar{N} = 100$. The $\bar{N}$ dependence in the revival times is as well a general feature as argued above; large $\bar{N}$ values imply long revival times [33]. In plot (a), a sequence of collapse-revivals appears; however, they are less clear as time progresses. For t plot (b), on the other hand, only a single collapse period is visible. When the time spans of revivals begin to overlap, which starts to happen after roughly 1 ms in (a) and already after the first revival in (b), super-revivals may occur due to higher order interferences [36]. Slight signatures of super-revivals can be seen in (b) in the modulated oscillations after $t \sim 10$. We note that for the present results, the time spans are of the same order as those for single Josephson oscillations in Fig. 10, this derives from the much weaker pump amplitude η in these examples giving a lower barrier between the two wells, i.e., shorter tunneling times.

As pointed out in the mean-field section, we have neglected effects arising from atom-atom nonlinearities by letting $g = 0$. The quadratic terms in atom numbers are known to render collapse-revivals [5,34], and with both nonlinearities present (atom-atom and atom-field interactions) one would see a competition between the two mechanisms. In general, revivals become less frequent, since they are only possible when both effects simultaneously support revivals. We have verified these conclusions numerically by including atom-atom interactions into our calculations.

The analysis of this section relies on a static assumption, i.e., the effective potential is considered independent of time. The collapse-revival structure is solely an outcome of the uncertainty of atom number and not of the instantaneous state of the atoms. The full time-dependent many-body problem is certainly interesting, but in this work we focus on general interesting phenomena inherent in the atom-field nonlinearity. Even though the results of these sections have been derived within some assumptions, we believe that the general structure survives also in more rigorous analyses. Such approaches would, for example, reveal how the steady-state photon number $n_{\rm ss} = \langle \hat{n}_{\rm ss} \rangle$ evolves in time. Nevertheless, it is believed that $n_{\rm ss}$ encodes the properties of the atomic evolutions exactly as it did in the previous section studying mean-field dynamics. That is, one would expectedly find a similar collapse-revival pattern in $n_{\rm ss}$ as the one found in the atomic inversion.

It is important to note that the collapse-revival phenomenon is a pure quantum effect. By adding fluctuations around the means $\Psi(x)$ of the previous two sections, one would typically encounter a collapse in the oscillations. However, the revivals depend strongly on the particular N dependence of $t(N)$, and therefore random fluctuations around $\Psi(x)$ would not predict revivals. In other words, capturing the revival structure from some perturbed mean-field approach is only possible if one could carefully choose the perturbing fluctuations.

VI. CONCLUSIONS

Nonlinear Josephson oscillations have been studied in a DW system of ultracold bosonic atoms. Contrary to regular nonlinearity, arising from atom-atom interaction in these types of systems, the nonlinearity we considered derives from intrinsic interaction between the atoms and a quantized cavity field. In particular, we demonstrated the appearance of pseudo-self-trapping, self-organization, as well as collapse-revivals. In other words, the present work shows that these phenomena are rather general and not restricted to only certain kinds of nonlinearities.

The system parameters were chosen in agreement with current experiments, indicating that the phenomena should be experimentally realizable. We furthermore showed or argued that the output cavity field, proportional to $n_{\rm ss}$, provides a direct handle of the atomic dynamics. Since the output field is regarded as losses, measurement of it is nondemolition by nature. Hence, the various evolution regimes can be traced down without standard destructive measurements such as time-of-flight or fluorescence detection.

ACKNOWLEDGMENTS

J.L. acknowledges support from the MEC program (FIS2005-04627) and VR/Vetenskapsrådet. We thank Anssi Collin, Maciej Lewenstein, Duncan O'Dell, Giovanna Morigi, and Jakob Reichel for insightful discussions.

[1] E. Hanamura, Y. Kawabe, and A. Yamanaka, *Quantum Nonlinear Optics* (Springer Verlag, Berlin-Heidelberg, 2007).

[2] C. Pethick and H. Smith, *Bose-Einstein Condensation in Dilute Gases* (Cambridge University, Cambridge, 2002).

[3] M. Greiner, O. Mandel, T. Esslinger, T. W. Hänsch, and I. Bloch, Nature (London) **415**, 39 (2002).

[4] L. Khaykovich, F. Schreck, G. Ferrari, T. Bourdel, J. Cubizolles, L. D. Carr, Y. Castin, and C. Salomon, Science **296**, 1290 (2002); K. W. Madison, F. Chevy, W. Wohlleben, and J. Dalibard, Phys. Rev. Lett. **84**, 806 (2000).

[5] G. J. Milburn, J. Corney, E. M. Wright, and D. F. Walls, Phys. Rev. A **55**, 4318 (1997).

[6] A. Smerzi, S. Fantoni, S. Giovanazzi, and S. R. Shenoy, Phys. Rev. Lett. **79**, 4950 (1997); S. Raghavan, A. Smerzi, S. Fantoni, and S. R. Shenoy, Phys. Rev. A **59**, 620 (1999).

[7] B. D. Josephson, Phys. Lett. **1**, 251 (1962); A. Barone and G. Paterno, *Physics and Applications of the Josephson Effect* (Wiley-VCH, New York, 1982).

[8] L. Radzihovsky and V. Gurarie, Phys. Rev. A **81**, 063609 (2010).

[9] O. Arcizet, P. F. Cohadon, T. Briant, M. Pinard, and A. Heidmann, Nature **444**, 71 (2006); T. J. Kippenberg and K. J. Vahal, Science **321**, 1172 (2008); F. Marquardt and S. M. Girvin, Physics **2**, 40 (2009).

[10] Y. Colombe, T. Steinmetz, G. Dubois, F. Linke, D. Hunger, and J. Reichel, Nature **450**, 272 (2007); F. Brennecke, T. Donner, S. Ritter, T. Bourdel, M. Kohl, and T. Esslinger, *ibid.* **450**, 268 (2007).

[11] F. Brennecke, S. Ritter, T. Donner, and T. Esslinger, Science **322**, 235 (2008).

[12] J. Larson, G. Morigi, and M. Lewenstein, Phys. Rev. A **78**, 023815 (2008); J. M. Zhang, F. C. Cui, D. L. Zhou, and W. M. Liu, *ibid.* **79**, 033401 (2009); L. Zhou, H. Pu, H. Y. Ling, and W. Zhang, Phys. Rev. Lett. **103**, 160403 (2009).

[13] S. Gupta, K. L. Moore, K. W. Murch, and D. M. Stamper-Kurn, Phys. Rev. Lett. **99**, 213601 (2007); K. W. Murch, K. L. Moore, S. Gupta, and D. M. Stamper-Kurn, Nature Phys. **4**, 561 (2008); S. Ritter, F. Brennecke, K. Baumann, T. Donner, C. Guerlin, and T. Esslinger, Appl. Phys. B **95**, 213 (2009).

[14] C. Maschler and H. Ritsch, Phys. Rev. Lett. **95**, 260401 (2005); J. Larson, B. Damski, G. Morigi, and M. Lewenstein, *ibid.* **100**, 050401 (2008); C. Maschler, I. B. Mekhov, and H. Ritsch, Eur. Phys. J. D **46**, 545 (2008); G. Chen, X. G. Wang, J. Q. Liang, and Z. D. Wang, Phys. Rev. A **78**, 023634 (2008).

[15] J. Larson, S. Fernández-Vidal, G. Morigi, and M. Lewenstein, New J. Phys. **10**, 045002 (2008).

[16] D. Nagy, G. Szirmai, and P. Domokos, Eur. Phys. J. D **48**, 127 (2008); S. Fernández-Vidal, G. De Chiara, J. Larson, and G. Morigi, Phys. Rev. A **81**, 043407 (2010).

[17] D. Nagy, G. Konya, G. Szirmai, and P. Domokos, Phys. Rev. Lett. **104**, 130401 (2010); K. Baumann, C. Guerlin, F. Brennecke, and T. Esslinger, Nature **464**, 1301 (2010).

[18] J. M. Zhang, W. M. Liu, and D. L. Zhou, Phys. Rev. A **77**, 033620 (2008); **78**, 043618 (2008).

[19] J. F. Corney and G. J. Milburn, Phys. Rev. A **58**, 2399 (1998).

[20] M. Albiez, R. Gati, J. Fölling, S. Hunsmann, M. Cristiani, and M. K. Oberthaler, Phys. Rev. Lett. **95**, 010402 (2005); S. Levy, E. Lahoud, I. Shomroni, and J. Steinhauer, Nature **449**, 579 (2007).

[21] C. J. Hood, T. W. Lynn, A. C. Doherty, A. S. Parkins, and H. J. Kimble, Science **287**, 1447 (2000).

[22] J. Larson, J. Mod. Opt. **53**, 1867 (2006).

[23] H. J. Carmichael, *An Open System Approach to Quantum Optics* (Springer Verlag, Berlin, 1993).

[24] D. Nagy, P. Domokos, A. Vukics, and H. Ritsch, Eur. Phys. J. D **55**, 659 (2009).

[25] P. Venkatesh, J. Larson, and D. O'Dell (unpublished).

[26] P. Horak and H. Ritsch, Phys. Rev. A **63**, 023603 (2001).

[27] H. Feshbach, Ann. Phys. (NY) **5**, 357 (1958); E. Tiesinga, B. J. Verhaar, and H. T. C. Stoof, Phys. Rev. A **47**, 4114 (1993).

[28] P. Domokos and H. Ritsch, Phys. Rev. Lett. **89**, 253003 (2002).

[29] J. K. Asboth, P. Domokos, H. Ritsch, and A. Vukics, Phys. Rev. A **72**, 053417 (2005).

[30] R. Graham and H. Haken, Z. Phys. **237**, 31 (1970); V. DiGiorgio and M. O. Scully, Phys. Rev. A **2**, 1170 (1970).

[31] M. D. Reed, L. DiCarlo, B. R. Johnson, L. Sun, D. I. Schuster, L. Frunzio, and R. J. Schoelkopf, e-print arXiv:1004.4323; L. S. Bishop, E. Ginossar, and S. M. Girvin, Phys. Rev. Lett. **105**, 100505 (2010).

[32] I. B. Mekhov, C. H. Maschler, and H. Ritsch, Nature Phys. **3**, 319 (2007); Phys. Rev. A **76**, 053618 (2007); B. Prasanna Venkatesh, M. Trupke, E. A. Hinds, and D. O'Dell, Phys. Rev. A **80**, 063834 (2009).

[33] S. Haroche and J.-M. Raimond, *Exploring the Quantum* (Oxford University, Oxford, 2006); M. S. Scully and Zubairy, *Quantum Optics* (Cambridge University, Cambridge, 1997).

[34] R. W. Robinett, Phys. Rep. **392**, 1 (2004).

[35] P. L. Knight and B. Shore, J. Mod. Opt. **40**, 1195 (1993); J. Larson, Phys. Scripta **76**, 146 (2007).

[36] D. Wang, T. Hansson, Å. Larson, H. O. Karlsson, and J. Larson, Phys. Rev. A **77**, 053808 (2008).